Molecular Vision 2015; 21:487-501 <http://www.molvis.org/molvis/v21/487>
Received 18 January 2015 | Accepted 26 April 2015 | Published 28 April 2015

Clinical presentations of X-linked retinoschisis in Taiwanese patients confirmed with genetic sequencing

Nan-Kai Wang,[1,2] Laura Liu,[1,2] Ho-Min Chen,[1,2] Shawn Tsai,[3,4] Tsong-Chi Chang,[5] Tzu-Hsun Tsai,[6,7] Chung-May Yang,[6,7] An-Ning Chao,[1,2] Kuan-Jen Chen,[1,2] Ling-Yuh Kao,[1,2] Ling Yeung,[2,8] Lung-Kun Yeh,[1,2] Yih-Shiou Hwang,[1,2] Wei-Chi Wu,[1,2] Chi-Chun Lai[1,2]

(The first two authors contributed equally to this work.)

[1]Department of Ophthalmology, Chang Gung Memorial Hospital, Linkou Medical Center, Taoyuan, Taiwan; [2]College of Medicine, Chang Gung University, Taoyuan, Taiwan; [3]Department of Ophthalmology, Mackay Memorial Hospital, Taipei, Taiwan; [4]Department of Optometry, Chung Shan Medical University, Taichung, Taiwan; [5]Department of Ophthalmology, Mackay Memorial Hospital, Hsinchu, Taiwan; [6]Department of Ophthalmology, National Taiwan University Hospital, Taipei, Taiwan; [7]Department of Ophthalmology, National Taiwan University Hospital; College of Medicine, National Taiwan University, Taipei, Taiwan; [8]Department of Ophthalmology, Chang Gung Memorial Hospital, Keelung, Taiwan

Purpose: To investigate the clinical characteristics of X-linked retinoschisis (XLRS) and identify genetic mutations in Taiwanese patients with XLRS.

Methods: This study included 23 affected males from 16 families with XLRS. Fundus photography, spectral domain optical coherent tomography (SD-OCT), fundus autofluorescence (FAF), and full-field electroretinograms (ERGs) were performed. The coding regions of the *RS1* gene that encodes retinoschisin were sequenced.

Results: The median age at diagnosis was 18 years (range 4–58 years). The best-corrected visual acuity ranged from no light perception to 20/25. The typical spoke-wheel pattern in the macula was present in 61% of the patients (14/23) while peripheral retinoschisis was present in 43% of the patients (10/23). Four eyes presented with vitreous hemorrhage, and two eyes presented with leukocoria that mimics Coats' disease. Macular schisis was identified with SD-OCT in 82% of the eyes (31/38) while foveal atrophy was present in 18% of the eyes (7/38). Concentric area of high intensity was the most common FAF abnormality observed. Seven out of 12 patients (58%) showed electronegative ERG findings. Sequencing of the *RS1* gene identified nine mutations, six of which were novel. The mutations are all located in exons 4–6, including six missense mutations, two nonsense mutations, and one deletion-caused frameshift mutation.

Conclusions: XLRS is a clinically heterogeneous disease with profound phenotypic inter- and intrafamiliar variability. Genetic sequencing is valuable as it allows a definite diagnosis of XLRS to be made without the classical clinical features and ERG findings. This study showed the variety of clinical features of XLRS and reported novel mutations.

X-linked retinoschisis (XLRS, OMIM 312700) is one of the most common causes of juvenile macular degeneration that affects males early in life. The major symptom is early onset of visual loss, and the typical presentations include radiating cystic changes of the macula with or without peripheral retinoschisis. Some patients may present with vitreous hemorrhage and retinal detachment.

In 1898, Hass first described two brothers with typical radiating cystic maculopathy and peripheral choroidal atrophy as "Veränderungen der Retina und Choroidea (English: Changes of the retina and choroid)" [1]. Since then, the disease has been diagnosed based on ophthalmoscopy and described in the literature under a wide variety of names according to different clinical manifestations and etiologies.

In the 1960s, abnormal electroretinograms (ERGs) was reported in XLRS [2-4], and the b/a ratio has been found to be abnormal in almost all cases [4,5]. Since then, electronegative ERG has been considered a typical finding in XLRS, and ERG has become an important examination for this disease. Recently, advanced retinal imaging including optical coherence tomography (OCT) and fundus autofluorescence (FAF) have been used to identify the typical features and have become important diagnostic tools for patients with XLRS. Although the initial underlying biologic abnormality in XLRS was thought to be Müller cells based on the histopathology [6] and electrophysiology [7], it was not until 1997 that the *RS1* gene (Gene ID: 6247; OMIM: 312700) was identified through the use of positional cloning [8].

Since XLRS is a recessive disease caused by a mutation in the *RS1* gene that encodes retinoschisin, gene therapy has

Correspondence to: Nan-Kai Wang, Department of Ophthalmology, Chang Gung Memorial Hospital, No. 5, Fu-Hsing Street, Kuei Shan, Taoyuan, 333, Taiwan; Phone: 886-3-3281200, ext. 8666; FAX: 886-3-3287798; email: wang.nankai@gmail.com

been considered a potential treatment for the near future. For couples with XLRS with confirmed mutation, preimplantation genetic diagnosis can help to selectively implant embryos without genetic defects using in vitro fertilization techniques. Therefore, diagnosing patients with XLRS correctly based on various clinical characteristics is important.

The purpose of this study was to examine the clinical characteristics of *RS1* in Taiwanese patients with XLRS and to further identify genetic mutations with genetic analysis. More specifically, we explored the relationship of the *RS1* genotype with various phenotypic features including symptoms, signs, and current ophthalmic examinations, such as fundus photography, FAF, OCT, and ERG.

METHODS

Patients: Twenty-three male patients from 16 families were recruited from our clinics. They were all of unexceptional health except eye disease with widely varying age. The diagnosis of XLRS was made clinically and based on the presence of macular schisis (with or without peripheral retina schisis changes) and electrophysiological findings, and then the diagnosis was confirmed using genetic screening for the *RS1* gene. This study was conducted with the approval of the Institutional Review Board (protocol No. 99–1063B) of Chang Gung Memorial Hospital, and the study followed the protocols of the Declaration of Helsinki. Informed consent was obtained from all participants after a full explanation of the nature and possible consequences of the study was provided.

Ophthalmic examinations: Patients underwent ophthalmic examinations including best-corrected visual acuity (BCVA), fundus photography, FAF imaging, spectral domain OCT (SD-OCT), and full-field ERG. Fundus photography was performed using a digital fundus camera (Nonmyd-α-DIII, Kowa Optimed, Chou-ku, Japan).

Fundus autofluorescence imaging and fluorescence angiography: FAF examinations were conducted using a confocal scanning laser ophthalmoscope (Heidelberg Retina Angiograph, Heidelberg Engineering, Heidelberg, Germany). Automated eye tracking and image alignment allowed for better resolution. One patient (patient N;II-1) received the fluorescent angiography (FA) examination using the Heidelberg Retina Angiograph.

Optical coherence tomography: SD-OCT images were obtained using either a Spectralis HRA-OCT (Heidelberg, Germany) or RTVue (Optovue, Inc., Fremont, CA). In cases with macular edema treated with topical dorzolamide, the OCT images were compared for morphological changes using the same machines.

Electroretinography: Full-field ERGs were performed using Burian-Allen contact lens electrodes as described previously [9]. Stimuli were generated with a commercial recording unit (Utas-E3000; LKC Technologies, Inc., Gaithersburg, MD) using standards from the International Society for Clinical Electrophysiology of Vision (ISCEV) [10], which included dark-adapted (DA) responses to flash intensity of 0.01 and 3.0 $cd.s.m^{-2}$ (DA 0.01 and DA 3.0) and light-adapted (LA) response to a flash intensity of 3.0 $cd.s.m^{-2}$ (LA 3.0) and 30 Hz flicker.

Genetic examinations: The coding region of *RS1* (exons 1–6) was sequenced for disease-causing mutations in all participants. DNA was extracted from peripheral blood using the QIAamp DNA Mini Kit (Qiagen Inc., Valencia, CA) as described elsewhere [9,11]. Extracted genomic DNA was amplified with polymerase chain reaction (PCR) with a MyCycler Thermal Cycler (Bio-Rad, Hercules, CA) using primer sequences as described in Table 1 [8,12]. The cycling conditions were an initial 10-min incubation at 95 °C, 35 cycles of 30 s at 95 °C, 30 s at 55 °C, and 1 min at 72 °C, and a final step of 7 min at 72 °C. The coding regions of the *RS1* gene that encode retinoschisin were directly sequenced after purification.

RESULTS

Clinical examinations: Table 2 and the Figure 1 and Figure 2 show the demographic, clinical, and genetic characteristics of the 23 patients. The median age at diagnosis was 18 years (range 4–58 years). The BCVA ranged from no light perception to 20/25. Eighteen of the 23 patients (78%) presented with decreased visual acuity, three patients with leukocoria, one patient with strabismus, and one with photophobia. Of the three patients (13%) with leukocoria, one was due to congenital cataract (M,II-1), one to Coats'-like exudation of the retina (M,II-3, Figure 2A), and one to total exudative retinal detachment with neovascular glaucoma, which was initially diagnosed as Coats' disease (G,III-6).

All patients had fundus abnormalities on indirect ophthalmoscopy. Fourteen of the 23 patients (61%) had a typical spoke-wheel pattern in the macula (Figure 2B), one patient had subretinal fibrosis (Figure 2G), and one patient had macula atrophy (Figure 2F) mimicking maculopathy. Vitreous hemorrhages were present in four patients (17%; B,II-1; D,II-1; I,II-1; M,II-1, mean age: 9 years), and all four patients had peripheral retinoschisis. Peripheral retinoschisis was present in ten patients (43%; Figure 2C,D,G,H,K), and peripheral pigmentary changes were observed in five patients

(22%; Figure 2D,H,J,K). A golden-yellow reflex was seen in patient K,II-1 (Figure 2I). Two patients had white dots in the posterior fundus mimicking fundus albipunctatus (Figure 2B,K), and one patient had sheathed vessels (Figure 2D).

Fundus autofluorescence imaging and fluorescence angiography: FAF imaging was performed in six patients, and fluorescence angiography in one. One patient (Figure 3A) had a spoke-wheel pattern of hyper- and hypo-FAF, two patients had an irregularly shaped area of hyper- and hypo-FAF (Figure 3B), and three patients had concentric areas of hyper-FAF (Figure 3C,D). Patient N,II-1 was a referral case and presented with non-FA leakage cystoid macula edema (Figure 3D), which suggested XLRS as a possible diagnosis.

Optical coherence tomography: Thirty-eight eyes from 23 patients underwent SD-OCT examinations. Macular schisis was observed in 31 eyes (82%), and foveal atrophy was observed in seven eyes (18%). Bilateral foveal atrophy was seen in three older patients (mean age: 49 years; Figure 4B). Two patients had macular schisis in one eye and foveal atrophy in the other eye (H,II-1; N,II-1, Figure 4C). Two patients had schisis and a lamellar hole in one eye and macular schisis with no hole in the other eye (J,II-2; K,II-1, Figure 4E,F).

Seven patients received topical dorzolamide for macular schisis, and four (30.8%) of 13 eyes had a decreased central foveal thickness (Figure 5A–D). Patient J,II-5 (OD, Figure 5A, OS, Figure 5B) showed significant resolution of the schisis/cystoid macula edema 7 months after treatment with topical dorzolamide. Patient K, II-1 showed a positive response to treatment in his right eye (Figure 5C), while the other eye (lamellar hole, Figure 4F) showed no response. Patient M,II-1 had reduced macula thickness 3 months after treatment (Figure 5D).

Electroretinography: In total, 12 patients underwent ERGs (Figure 6, Figure 7). The DA 0.01 ERG was reduced in all patients, and the DA 3.0 ERG showed a reduced b/a ratio in all patients except patient L,II-1 (Figure 6). Seven patients (C,II-1; F,II-1; G,III-3; K,II-1; N,II-1; P,II-1; P,II-2) had a b/a ratio <1 on the DA 3.0 ERG, which achieved the definition of an electronegative ERG, while five patients had a b/a ratio >1. Patient L,II-1 showed a normal b/a ratio of >1, and the amplitudes of the a- and b-waves decreased.

All patients showed a delay in implicit time and a decrease in the amplitude of the b-wave in the LA 3.0 ERG. A delayed LA 30 Hz flicker peak time and decreased amplitude were observed in all patients (Figure 6, Figure 7).

Genetic studies: All patients had genetic mutations in the *RS1* gene, and the mutations were localized in exons 4, 5, and 6 encoding the discoidin domain. One deletion-caused frame-shift mutation was found in exon 5 (Family D), one nonsense mutation in exon 5 (Families L and E), one nonsense mutation in exon 6 (Families F, G, M, O, and P), and the rest were missense mutations (Table 2, Appendix 1). Among these nine mutations, three were known, and six were novel (Table 2, Appendix 1). The brother of patient J;II-2 was born using the technique of preimplantation genetic diagnosis. Multiple species sequence alignment of the portion of the discoidin domain showed that the mutation sites were highly conserved (see Figure 8).

DISCUSSION

This paper has reported the clinical characteristics, ERG features, and *RS1* gene mutations from 23 affected male patients from 16 Taiwanese families. Profound phenotypic inter- and intrafamiliar variability was noted.

Table 1. Primers for the *RS1* mutation analysis.

Gene	Exon	Primers	Sequence (5'-3')
RS1	1	F	CTCAGCCAAAGACCTAAGAAC
		R	GTATGCAATGAATGTCAATGG
	2	F	GTGATGCTGTTGGATTTCTC
		R	CAAAGTGATAGTCCTCTATG
	3	F	CTGCCCTGCCTCTCTGGTTG
		R	GGTGTTCCCAATGACTGTTCC
	4	F	GGTGCTTGTTGAGTATTGAG
		R	AAAATCCCCGGGCCCTGC
	5	F	GAGAGCCAGCACCTGCGG
		R	GGGTGCGAGCTGAAGTTGG
	6	F	CCCGATGTGATGGTGACAGG
		R	CTTTGTTCTGACTTTCTCTGGC

Table 2. Clinical Data of 23 Male Patients from 16 Taiwanese Families with XLRS.

Family	Case	Nucleotide change	Amino acid change	Age at Dx (y)	BCVA (OD; OS)	Macula abnormalities	Periph-eral RS	Vitreous hemorrhage	Retinal detachment	ERG Scot. Max. b/a ratio
A †	II-1	c.304 C>T	p.Arg102Trp	58	20/200; 20/200	Macular schisis	No	No	No	>1
B†	II-1	c.458 T>C #	p.Val153Ala	18	20/60;20/60	Macular schisis	Yes	Yes OD	No	>1
C†	II-1	c.335 G>C #	p.Trp112Ser	23	20/200; 20/200	Macula schisis OD RPE atrophy OS	Yes OD	No	No	<1
D ‡	II-1	c.327_410del #	p.Cys110_ Leu137del	6	HM; 20/50	Macular schisis	Yes OU	Yes OU	Surgery for severe PVR OD	Not tested
E*	II-1	c.488 G>A #	p.Trp163Ter	6	20/60; 20/50	Macular schisis	No	No	No	Not tested
F*	I-2	c.531 T>G #	p.Tyr177Ter	52	20/1000; 20/1000	RPE atrophy	No	No	No	>1
F*	II-1	c.531 T>G #	p.Tyr177Ter	42	20/200; 20/200	Macular schisis	Yes OD	No	No	<1
G*	I-1	c.531 T>G #	p.Tyr177Ter	72	20/200; 20/200	RPE atrophy	No	No	No	Not tested
G*	III-2	c.531 T>G #	p.Tyr177Ter	18	20/40; 20/40	Macular schisis	No	No	No	>1
G*	III-3	c.531 T>G #	p.Tyr177Ter	17	LP; 20/60	Macular schisis OS	Yes OS	No	Phthisis after surgery for severe/PVR OD	<1
G*	III-6	c.531 T>G #	p.Tyr177Ter	5	NLP; 20/25	Macular schisis OS	No	No	NVG and Coats'-like appearance OD	Not tested
H †	II-1	c.214 G>A	p.Glu72Lys	6	20/200; 20/400	Macular schisis OD RPE atrophy OS	Yes OS	No	Subretinal fibrosis OS	Not tested
I†	II-1	c.304 C>T	p.Arg102Trp	5	20/1000; 20/2000	Macular schisis	Yes	Yes	Exudation	Not tested
J†	II-2	c.461 A>C #	p.Gln154Pro	5	Not tested	Macular schisis Hole OS	No	No	No	Not tested
J†	II-5	c.461 A>C	p.Gln154Pro	10	20/40; 20/30	Macular schisis	No	No	No	Not tested
K †	II-1	c.304 C>T	p.Arg102Trp	22	20/200; 20/200	Macular schisis Hole OS	No	No	No	<1
L*	II-1	c.488 G>A #	p.Trp163Ter	11	20/60;20/60	Macular schisis	No	No	No	>1, normal
M*	II-3	c.531 T>G#	p.Tyr177Ter	4	LP; 20/300	Macular schisis OS	No	No	Coats'-like appearance OD	Not tested
M*	II-1	c.531 T>G #	p.Tyr177Ter	7	No LP; 20/300	Macular schisis OS	Yes	Yes OS	Yes OS Phthisis OD	Not tested
N†	II-1	c.626 G>A	p.Arg209His	51	20/200; 20/60	Macular schisis OD RPE atrophy OS	No	No	No	<1
O*	II-1	c.531 T>G #	p.Tyr177Ter	30	20/30; 20/30	Macular schisis	No	No	No	<1

Family	Case	Nucleotide change	Amino acid change	Age at Dx (y)	BCVA (OD; OS)	Macula abnormalities	Periph-eral RS	Vitreous hemorrhage	Retinal detachment	ERG Scot. Max. b/a ratio
P*	II-1	c.531 T>G #	p.Tyr177Ter	41	CF; 20/200	Macular schisis OS	Yes	No	Yes	<1
P*	II-2	c.531 T>G #	p.Tyr177Ter	31	CF; 20/100	Macular schisis OS	Yes	No	Surgery for severe PVR OD	Not tested

VA: visual acuity; BCVA: best-corrected visual acuity; LP: light perception; HM: hand motion; CF: counting finger; RPE: retinal pigment epithelium; RS: retinoshisis; NVG: neovascular glaucoma; PVR: proliferative vitreoretinopathy; Scot.: scotopic; Max.: maximum. *: nonsense mutation; †: missense mutation, ‡: deletion related frame-shift, #: novel mutation.

Molecular Vision 2015; 21:487-501 <http://www.molvis.org/molvis/v21/487>

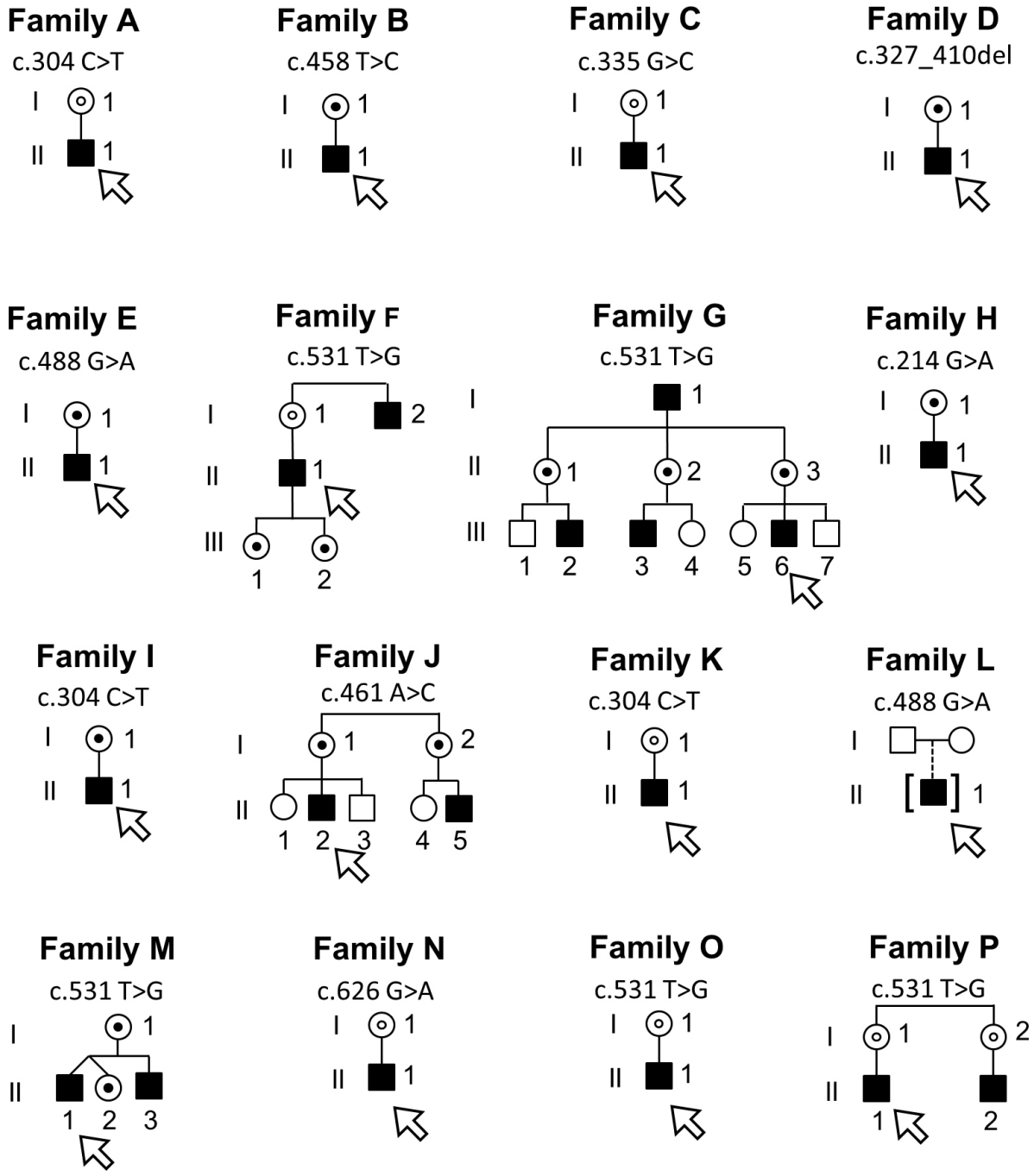

Figure 1. Pedigrees of 16 Taiwanese families with X-linked retinoschisis and identified mutations in the *RS1* gene. Black boxes represent affected males, and arrows point to probands. Circles with a black dot in the center represent carrier females by sequence analysis, while circles with an open dot represent non-tested potential carriers. Mutations of the *RS1* gene were screened for all family members except those who did not want to or could not participate in the study. Patient II-1 in Family L was adopted into the family with no previous family history available. Patient II-1 and II-2 in Family M were dizygotic twins.

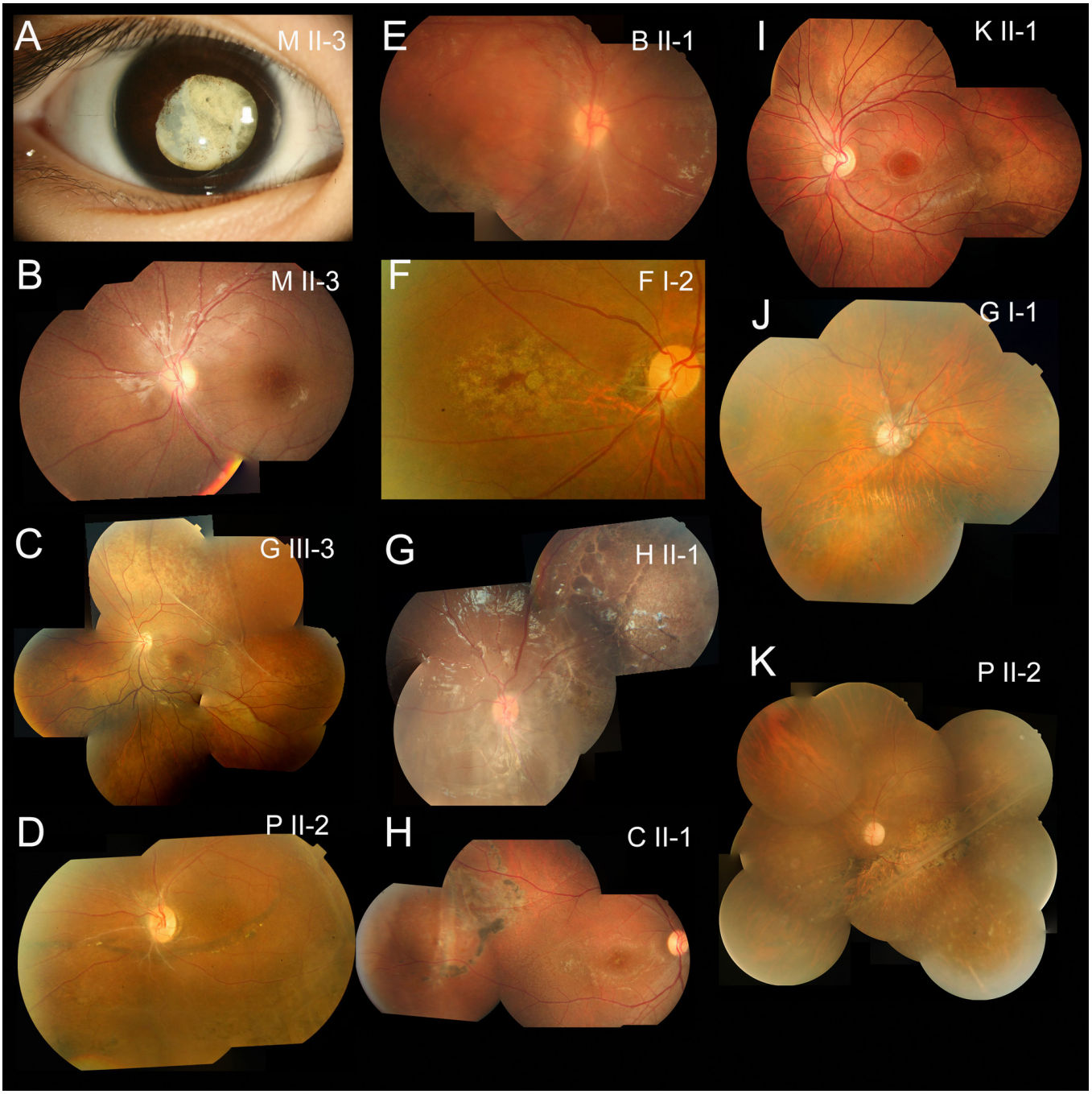

Figure 2. External and fundus photographs in patients with X-linked retinoschisis and identified mutations in the *RS1* gene. **A**: External photograph of patient M,II-3 (4 years) showed total lens opacification, and Coats' disease was suspected initially when he was young. **B**: Fundus photograph of patient M,II-3 (4 years) had a typical cartwheel-like appearance in the central macula and white spots in the posterior pole. **C**: Patient G,III-3 (17 years) had peripheral retinal splitting at the superior temporal area. **D**: Patient P,II-2 (31 years) had sheathed retinal vessels with retinal splitting and pigmentation. **E**: Patient B,II-1 (18 years) had mild vitreous hemorrhage. **F**: Patient F,I-2 (52 years) had macula atrophy. **G**: Patient H,II-1 (6 years) had subretinal fibrosis and peripheral retinal splitting. **H**: Patient C,II-1 (23 years) had peripheral splitting and pigmentation. **I**: Patient K,II-1 (22 years) had golden-yellow reflex at the temporal retina. **J**: Patient G,I-1 (72 years) had peripheral retinal pigmentation without splitting. He did not have myopia, so the peripapillary crescent may be related to age and may not be related to this disease. **K**: Patient P,II-2 (31 years) had retinal splitting across the macula and white dots at the inferior temporal retina.

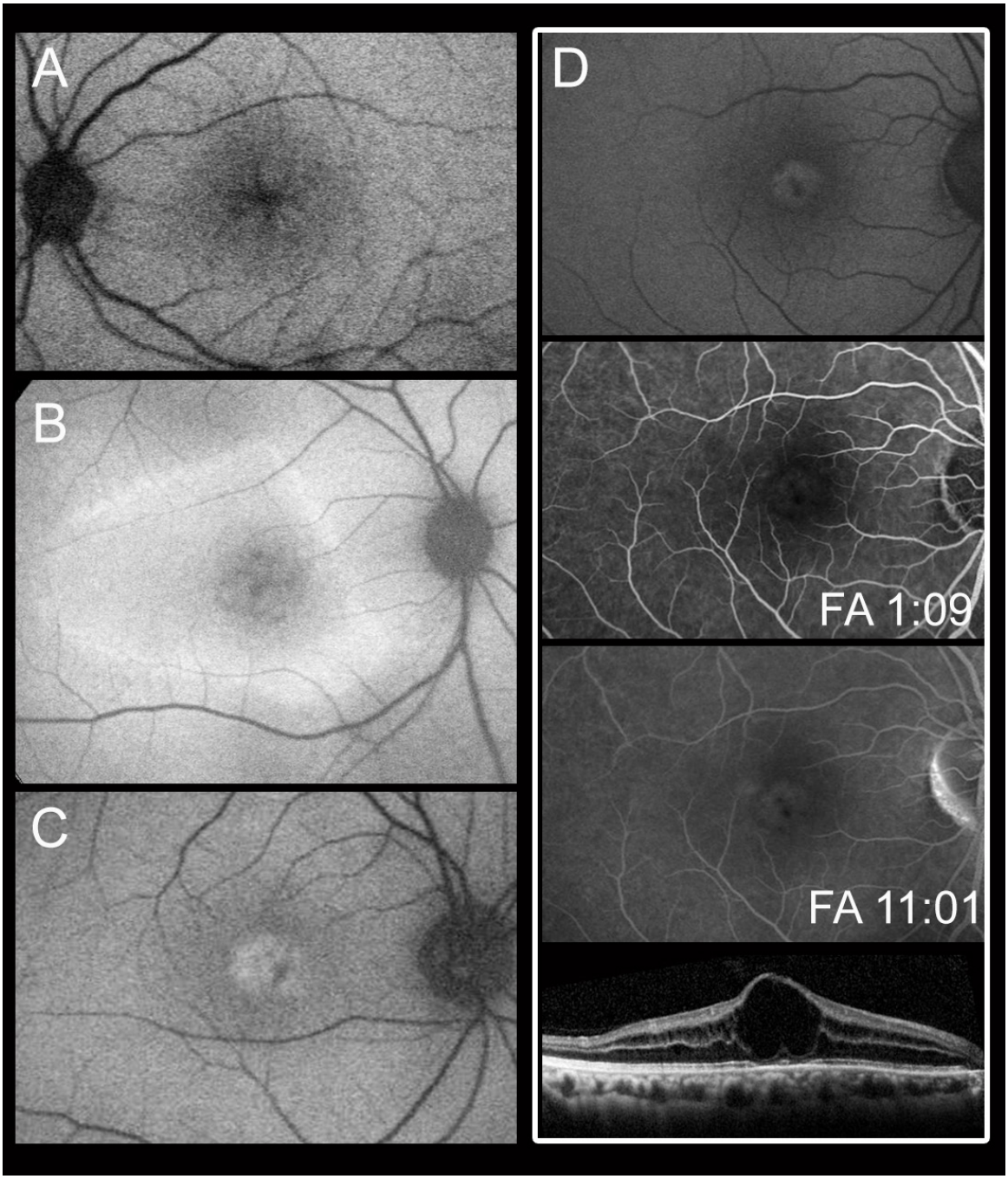

Figure 3. Fundus autofluorescence (FAF) and non-leakage cystoid macula edema in patients with X-linked retinoschisis. **A**: FAF for patient A,II-1 (58 years) showed a spoke-wheel pattern of hyper- and hypo-FAF in the macula area. **B**: Patient C,II-1 (23 years) had irregularly shaped areas of hyper- and hypo-FAF. **C**: Patient K,II-1 (22 years) had concentric areas of hyper-FAF. **D**: Patient N,II-1 (51 years) had concentric areas of hyper-FAF (upper), and fluorescence angiography (middle) revealed no leakage in the central macula, which corresponded to cystoid macula edema on spectral domain optical coherent tomography (bottom).

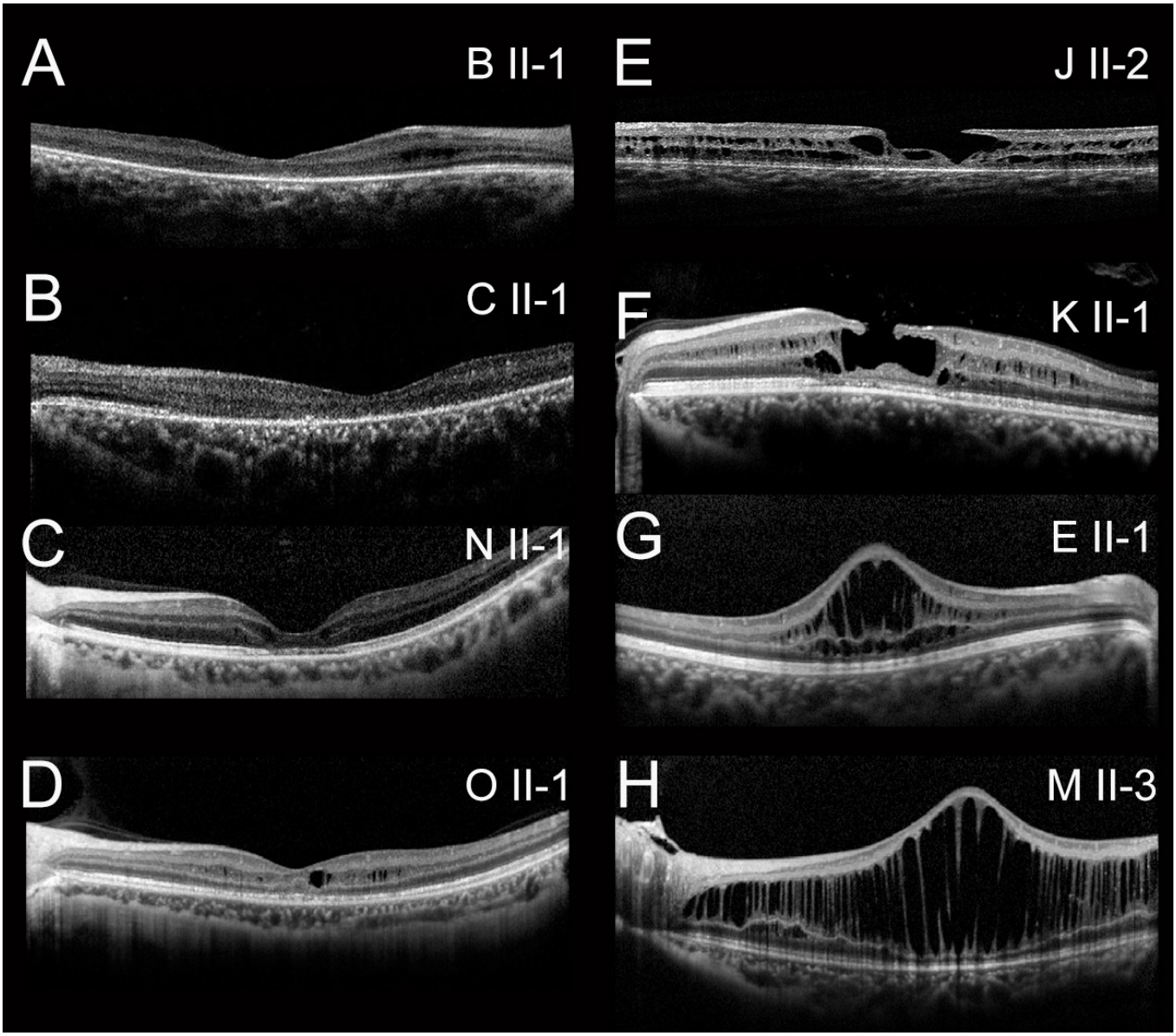

Figure 4. SD-OCT in patients with X-linked retinoschisis. **A**: Patient B,II-1 (18 years) had lamellar schisis. **B**: Patient C,II-1 (23 years) had photoreceptor and RPE atrophy in the fovea. **C**: Patient N,II-1 (51 years) had parafoveal schisis and foveal atrophy. **D**: Patient O,II-1 (30 years) had foveolamellar schisis. **E**: Patient J,II-2 (5 years) had foveolamellar schisis and lamellar hole. **F**: Patient K,II-1 (22 years; OS) had foveolamellar schisis and lamellar hole. **G**: Patient E,II-1 (6 years) had foveal schisis and increased thickness in the fovea. **H**: Patient M,II-3 (4 years) had foveolamellar schisis and increased thickness in the macula area.

Clinical features: Although a spoke wheel–like appearance in the macula is the most typical characteristic feature of XLRS, this feature may be obscured when there is a vitreous hemorrhage in a young patient or may be absent in older patients. Therefore, clinicians should suspect XLRS as one of the differential diagnoses in young boys who present with unsatisfactory BCVA with or without vitreous hemorrhage or leukocoria, because a sudden visual decrease in XLRS rarely occurs and is often associated with complications such as vitreous hemorrhage or retinal detachment. Diagnosis of XLRS in older patients or patients without macula schisis is also challenging because it may present with various fundus appearances, such as peripheral retinal pigmentation and macular atrophy.

Fundus autofluorescence imaging and fluorescence angiography: FAF is used for the differential diagnosis of retinal degeneration or dystrophy. The typical FAF finding in patients with XLRS is a spoke-wheel pattern of hyper- and

hypo-FAF in the macular area (Figure 3A), which is most likely due to changed light transmission in the area of retinoschisis [13]. However, in our study, three out of six patients (50%) presented with concentric areas of hyper-FAF (Figure 3C,D), which must be differentiated from other maculopathy or retinal dystrophies. Although fluorescence angiography is not required for the diagnosis of XLRS, FA may reveal nonleaking cystoid macular edema (Figure 3D), which may help clinicians better differentiate nicotinic acid toxicity, enhanced S-cone syndrome [11], and optic pit–related macular edema.

Optical coherence tomography: It has been suggested that retinoschisin functions as a cell adhesion protein to maintain the cellular organization of the retina and the structural integrity of the photoreceptor–bipolar synapse [13]. Mutation in the *RS1* gene may cause cystic cavity formation in different layers of the retina. OCT has become one of the most important examinations for patients with XLRS since Stanga et al.

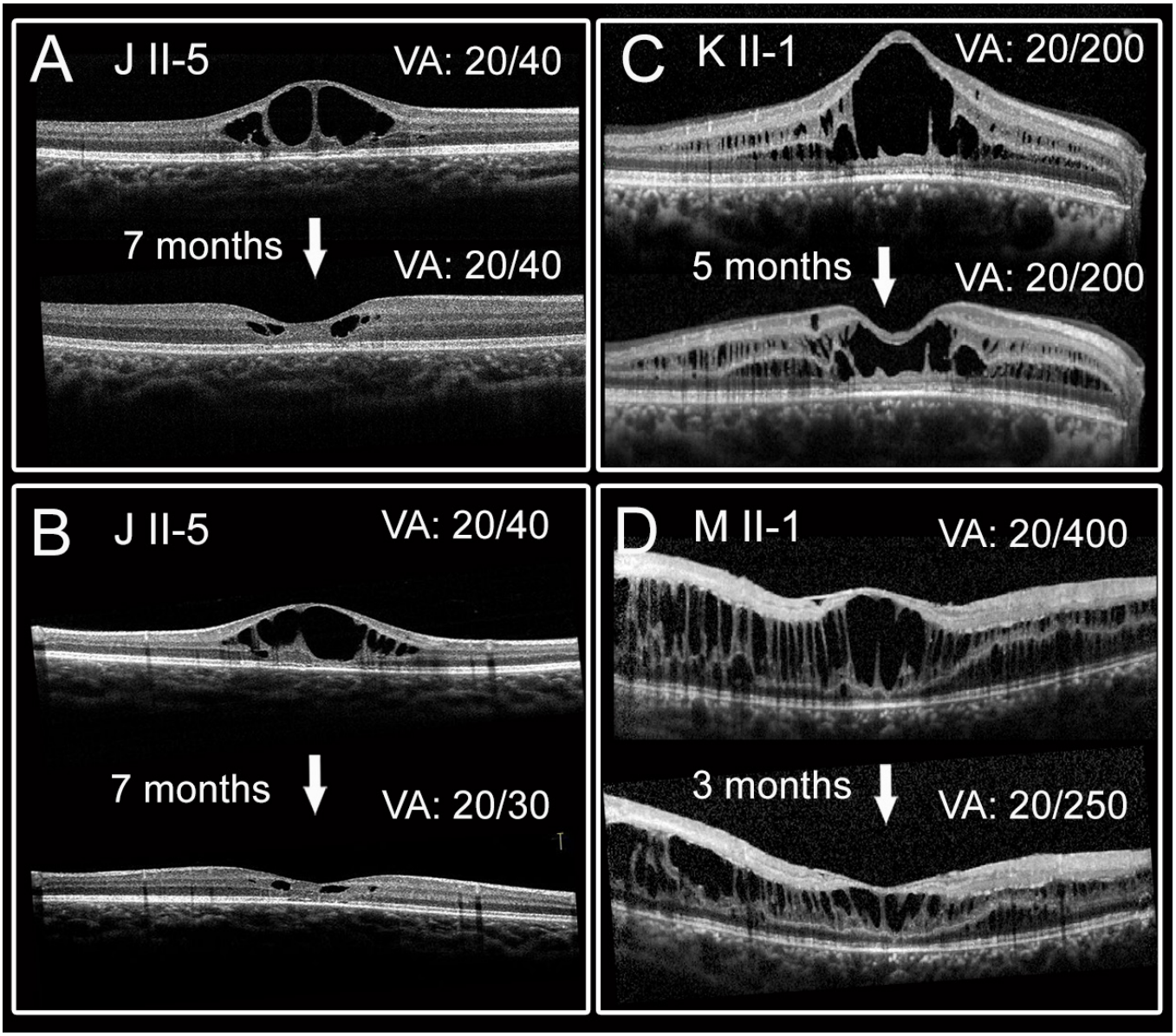

Figure 5. SD-OCT changes after treatment with topical dorzolamide solution. **A, B**: Patient J,II-5 (10 years) showed partial resolution of foveal cysts after topical dorzolamide treatment for 7 months, A: OD, B: OS. **C**: Patient K,II-1 (22 years) showed a positive response 5 months after topical dorzolamide treatment, while the other eye (lamellar hole, Figure 4F) showed no response. **D**: Patient M,II-1 (7 years) showed a decrease in central foveal thickness after topical dorzolamide treatment for 3 months.

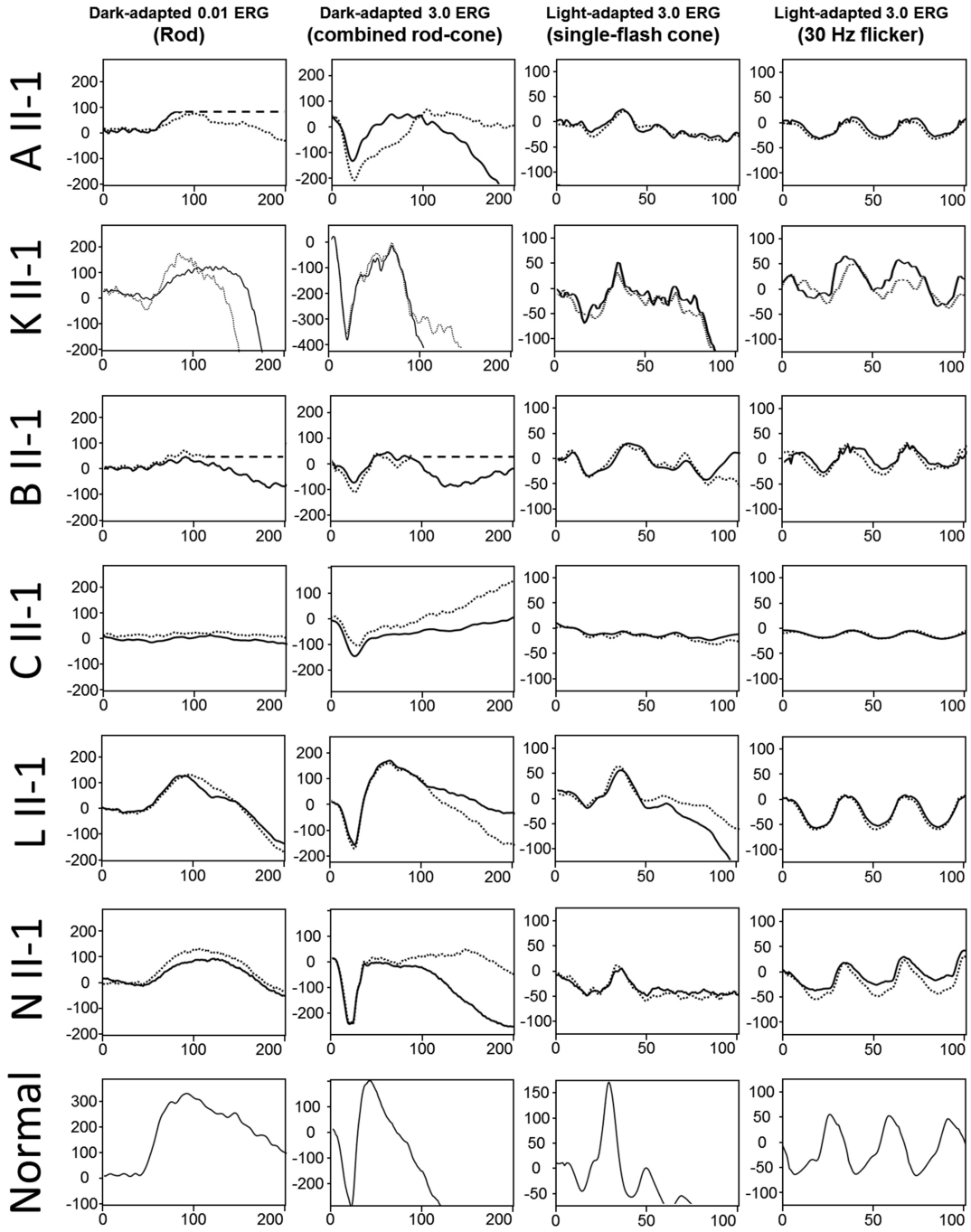

Figure 6. ERG from six patients and normal controls. The dark-adapted (DA) 0.01 electroretinogram (ERG) was reduced in all patients tested, and the DA 3.0 ERG showed a reduced b/a ratio in all patients tested except patient L; II-1 (11 years). Three patients [C,II-1 (23 years, c.335G>C); K,II-1 (22 years, c.304C>T); N,II-1 (51 years, c.626G>A)] showed a b/a ratio <1 on the DA 3.0 ERG, while the other three patients [A,II-1 (58 years, c.304C>T); B,II-1 (18 years, c.458T>C); L,II-1 (11 years, c.488G>A)] had a b/a >1. The light-adapted (LA) 3.0 ERG b-waves were delayed and decreased in amplitude in all patients tested. Delayed LA 30 Hz flicker peak time and decreased amplitude were observed in all patients. Solid lines represent average traces of the right eyes, and small dashed lines represent the average traces of the left eyes. Long dashed lines represent eye-blink artifacts [A,II-1 (58 years); B,II-1 (18 years)].

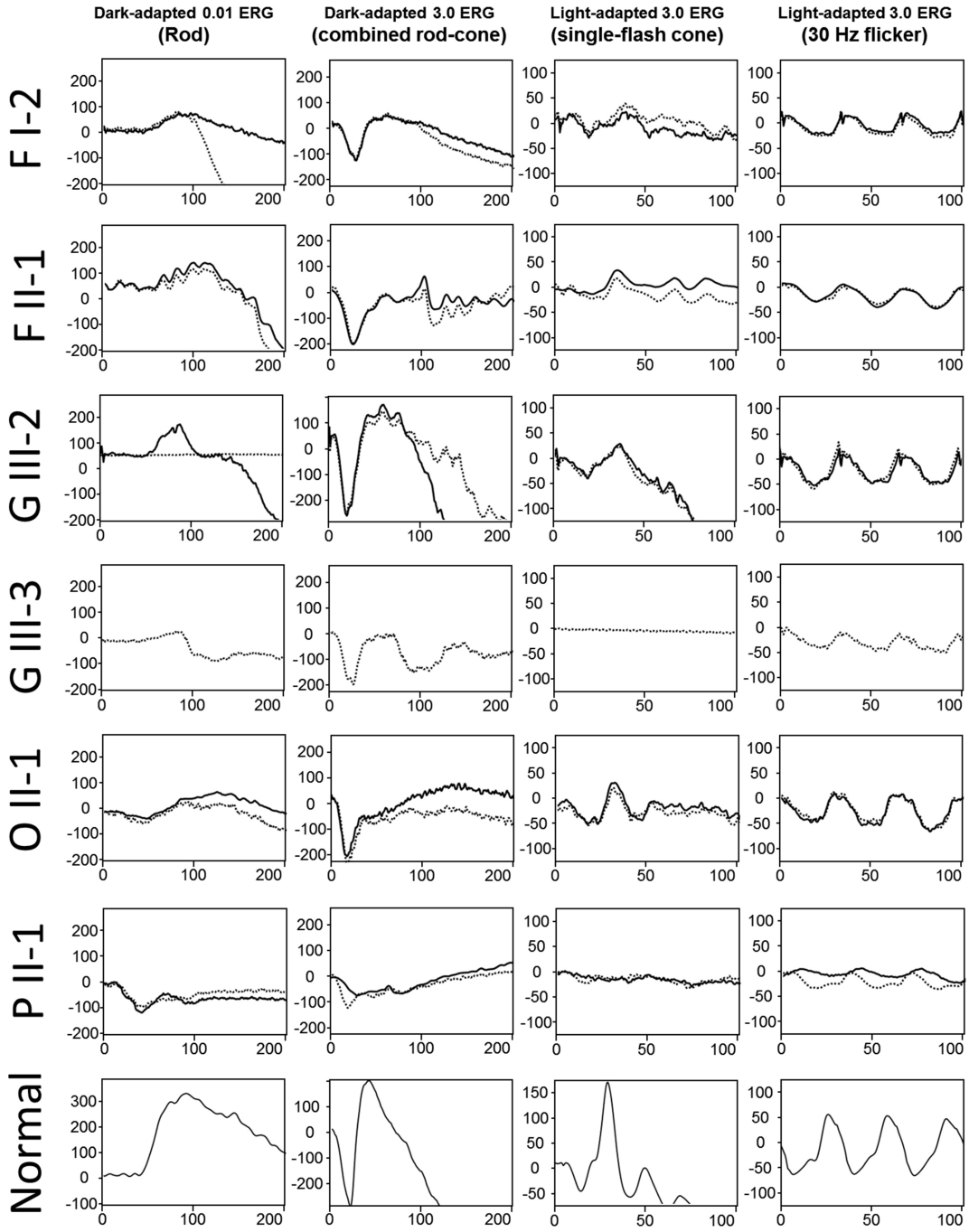

Figure 7. Electroretinograms (ERGs) from six patients with the same mutation (c.531T>G) and normal controls. Four patients [F,II-1 (42 years); G,III-3 (17 years); O,II-1 (30 years); P,II-1 (41 years)] showed a b/a ratio <1 on the DA 3.0 ERG, while the two other patients [F,I-2 (52 years); G,III-2 (18 years)] had a b/a >1. Only the left eye was tested (small dashed line) in patient G,III-3 (17 years) because the right eye had phthisical changes after vitreoretinal surgery for retinal detachment. Solid lines represent average traces of the right eyes, and small dashed lines represent the average traces of the left eyes.

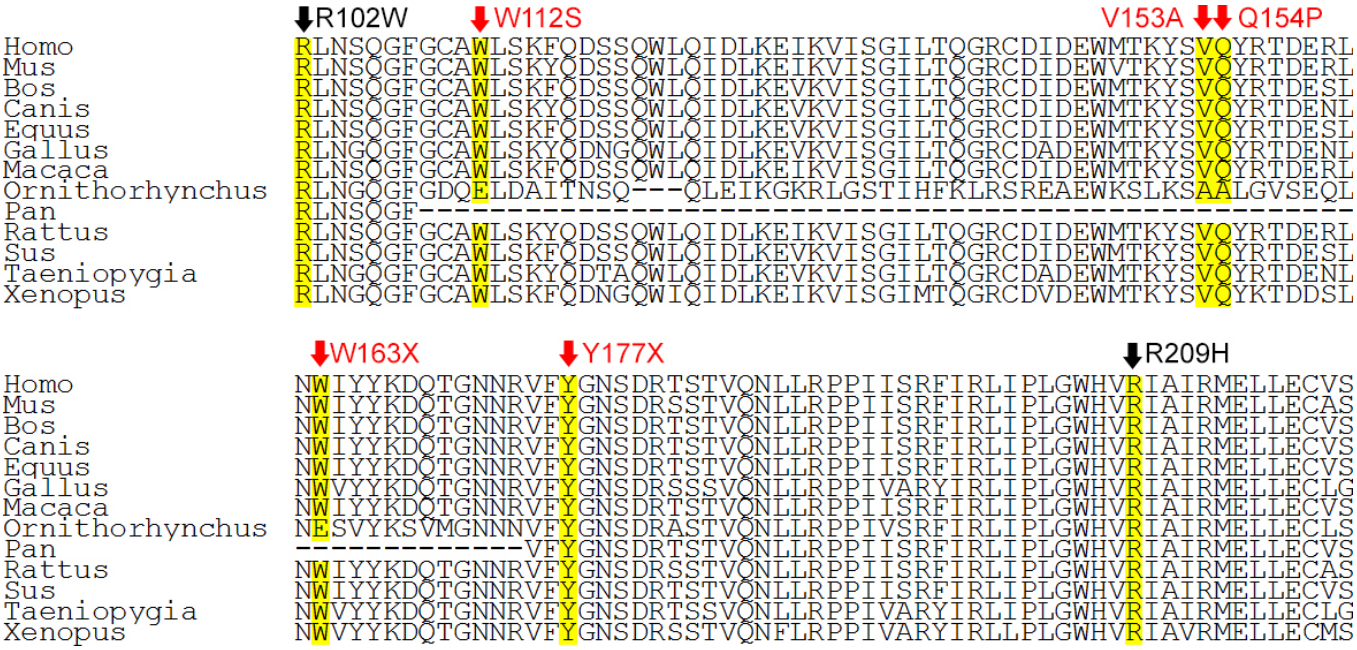

Figure 8. Multiple species sequence alignment of the portion of the discoidin domain. Multiple species sequence alignment of the portion of discoidin domain that spans the mutations showed that the mutation sites were highly conserved. Mutations in red are novel mutations that have never been reported, whereas mutations in black are not novel.

first demonstrated a cleavage plane in the neural retina [14], and since then, several classifications have been proposed based on clinical and OCT examinations [15,16]. Using SD-OCT, clinicians can easily evaluate young patients when dilated ophthalmoscopy and ERG are difficult to perform. Although cystoid macular edema is the typical OCT finding for patients with XLRS, intraretinal cysts with no increase in the thickness of the macula, macular lamellar holes, and RPE atrophy can also be present in patients with XLRS (Figure 4).

Genetic study and phenotype–genotype correlation: All the mutations in our study that were clustered in the discoidin domain occurred within conserved residues. Several studies have shown that mutation in the discoidin domain causes protein misfolding and retention in the endothelium reticulum, which subsequently results in the phenotype [17,18].

Similar to the results from studies intended to determine phenotype–genotype correlations [12,19,20], no phenotype–genotype correlation was found in our study. We also found intrafamilial variations (clinical features and electroretinography) in two families with the same mutations (Families F and G). From these findings, it is clear that the phenotypes in XLRS can be highly variable in individuals, and even within the same family.

Electroretinography: A “negative ERG” was originally defined by Karpe as a normal a-wave and a diminished b-wave [21]. In the last two decades, the definition has been expanded to include any ERG findings in which the amplitude of the b-wave is smaller than the a-wave [22]. Although an electronegative ERG has been historically considered characteristic of XLRS, seven out of 12 patients (58%) showed electronegative ERGs, which is consistent with a report by Renner et al. (56.5%) [23]. In addition, since one patient in our study (Figure 6L, II-1) showed a normal b/a ratio, a normal b/a ratio in DA 3.0 ERG does not exclude the diagnosis of XLRS.

Vincent et al. reported that nonsense, splice-site, or frame-shifting mutations in *RS1* consistently caused electronegative ERG in bright-flash (DA 11.0) stimuli, while missense mutations resulted in a wider range of ERG abnormalities [24]. In our study, seven patients with nonsense or deletion-related frameshift mutations underwent ERG; four had a b-wave smaller than the a-wave on the (DA 3.0) ERG (F,II-1, G,III-3, O,II-1, and P,II-1), and the other three had a b-wave larger than the a-wave on the (DA 3.0) ERG (F,I-2; G,III-2; L,II-1). This inconsistency may be related to the different bright flash intensities (DA 3.0 versus 11.0 ERG) used in the studies.

Dorzolamide for macular schisis/edema: Previous reports have shown that cystic macular lesions in XLRS may spontaneously resolve and further form an atrophic lesion in the macula [25,26]. Carbonic anhydrase inhibitors (CAIs) have

been reported to be effective for improving cystoid macular edema in patients with XLRS [27-30]. The clinical effect of CAIs has been demonstrated through modulation of membrane-bound carbonic anhydrase IV receptors present in the RPE layer [31]. The administration of CAIs has also been shown to enhance fluid transport in the RPE barrier and to enhance retinal adhesiveness [32].

Genead et al. reported that 20 of 29 eyes (69%) had a positive response to topical dorzolamide treatment and that 16 eyes of 12 patients (55%) had improvements in BCVA by at least seven letters in at least one eye during the most recent follow-up visit [29]. Khandhadia et al. also reported a positive response to the treatment, which was not related to genotype. However, this response did not correlate with improvements in visual acuity [28]. In our study, although four (30.8%) of 13 eyes showed a decrease in the central foveal thickness (Figure 4I–L), no eyes demonstrated clinically significant improvements in VA. Additional studies with a longer follow-up period on treating younger patients with XLRS are necessary to elucidate whether the treatment of cystic-like lesions can decrease the incidence of late-onset atrophic lesions or improve VA when treatment starts earlier.

In conclusion, XLRS is a clinically heterogeneous disease, and patients from a family with the same mutation (genotype) may have different phenotypes. Young boys can present with vitreous hemorrhage and exudative retinal detachment (RD), with or without neovascular glaucoma that mimics Coats' disease, and school-age boys may present with poor BCVA, amblyopia, or strabismus. Older patients, however, may present with retinal pigmentation or maculopathy, and not all patients show electronegative (scotopic maximal b/a <1) ERG. Although SD-OCT is a noninvasive, quick method for screening for the presence of macular schisis when dilated ophthalmoscopy and ERG are difficult to perform, XLRS may present as foveal atrophy in older patients. Although some patients have a positive response to topical dorzolamide, vision tends not to improve to a great extent. Although an electronegative (scotopic maximum b/a <1) ERG has been historically considered characteristic of XLRS, not all patients with XLRS have a negative ERG. Therefore, remaining highly aware of the possibility of XLRS and carrying out genetic testing for *RS1* gene mutations is still the best course of action for diagnosing XLRS and the identifying its carriers. To the best of our knowledge, this study is the first report of clinical and genetic features in Taiwanese patients with XLRS and provides information for timely genetic counseling and gene therapy in the future.

APPENDIX 1. SEQUENCES OF *RS1* MUTATIONS IDENTIFIED IN THIS STUDY.

To access the data, click or select the words "Appendix 1." Nine mutations were found in this study, including 6 missense, 2 nonsense, and 1 deletion-caused frame shift mutation. Six mutations in our study were novel.

ACKNOWLEDGMENTS

The authors thank Retinal Imaging and Electrophysiology Technicians (Department of Ophthalmology, Chang Gung Memorial Hospital, Linkou & Taipei) for technical assistance. NKW was supported by the National Science Council NSC-102–2314-B-182A-102-MY3 and the Chang Gung Memorial Hospital CMRPG 381803 & 3C1051. The funding organization had no role in the design or conduct of this research.

REFERENCES

1. Haas J. Ueber das Zusammenvorkommen von Veraenderungen der Retina und Choroidea. Arch Augenheilkd 1898; 39:343-8. .
2. Forsius H, Eriksson A, Valnio-Mattilla B. Geschlechtsgebundene erbliche Retinoschisis in zwei Familien in Finnland. Klin Monatsbl Augenheilkd 1963; 143:806-816. [PMID: 14115917].
3. Deutman AF. The hereditary dystrophies of the posterior pole of the eye [Ph.D. thesis]: Koninklijke Van Gorcum, Assen; 1971.
4. Hirose T, Wolf E, Hara A. Electrophysiological and Psychophysical Studies in Congenital Retinoschisis of X–Linked Recessive Inheritance. In: Lawwill T, editor. ERG, VER and Psychophysics. Vol 13: Springer Netherlands; 1977. p. 173–84.
5. Krill AE. Krill's Hereditary Retinal and Choroidal Diseases. Cambridge, London, New York: Harper & Row, Hagerstown; 1977.
6. Condon GP, Brownstein S, Wang NS, Kearns JA, Ewing CC. Congenital hereditary (juvenile X-linked) retinoschisis. Histopathologic and ultrastructural findings in three eyes. Arch Ophthalmol 1986; 104:576-83. [PMID: 3954665].
7. Peachey NS, Fishman GA, Derlacki DJ, Brigell MG. Psychophysical and electroretinographic findings in X-linked juvenile retinoschisis. Arch Ophthalmol 1987; 105:513-6. [PMID: 3566604].
8. Sauer CG, Gehrig A, Warneke-Wittstock R, Marquardt A, Ewing CC, Gibson A, Lorenz B, Jurklies B, Weber BH. Positional cloning of the gene associated with X-linked juvenile retinoschisis. Nat Genet 1997; 17:164-70. [PMID: 9326935].
9. Wang NK, Chuang LH, Lai CC, Chou CL, Chu HY, Yeung L, Chen YP, Chen KJ, Wu WC, Chen TL, Chao AN, Hwang YS. Multimodal fundus imaging in fundus albipunctatus with

RDH5 mutation: a newly identified compound heterozygous mutation and review of the literature. Doc Ophthalmol 2012; 125:51-62. [PMID: 22669287].

10. Marmor MF, Fulton AB, Holder GE, Miyake Y, Brigell M, Bach M. ISCEV Standard for full-field clinical electroretinography (2008 update). Doc Ophthalmol 2009; 118:69-77. [PMID: 19030905].
11. Wang NK, Fine HF, Chang S, Chou CL, Cella W, Tosi J, Lin CS, Nagasaki T, Tsang SH. Cellular origin of fundus autofluorescence in patients and mice with a defective NR2E3 gene. Br J Ophthalmol 2009; 93:1234-40. [PMID: 19429590].
12. Kim SY, Ko HS, Yu YS, Hwang JM, Lee JJ, Kim SY, Kim JY, Seong MW, Park KH, Park SS. Molecular genetic characteristics of X-linked retinoschisis in Koreans. Mol Vis 2009; 15:833-43. [PMID: 19390641].
13. Molday RS, Kellner U, Weber BH. X-linked juvenile retinoschisis: clinical diagnosis, genetic analysis, and molecular mechanisms. Prog Retin Eye Res 2012; 31:195-212. [PMID: 22245536].
14. Stanga PE, Chong NH, Reck AC, Hardcastle AJ, Holder GE. Optical coherence tomography and electrophysiology in X-linked juvenile retinoschisis associated with a novel mutation in the XLRS1 gene. Retina 2001; 21:78-80. [PMID: 11217940].
15. Prenner JL, Capone A Jr, Ciaccia S, Takada Y, Sieving PA, Trese MT. Congenital X-linked retinoschisis classification system. Retina 2006; 26:S61-4. [PMID: 16946682].
16. Lesch B, Szabo V, Kanya M, Somfai GM, Vamos R, Varsanyi B, Pamer Z, Knezy K, Salacz G, Janaky M, Ferencz M, Hargitai J, Papp A, Farkas A. Clinical and genetic findings in Hungarian patients with X-linked juvenile retinoschisis. Mol Vis 2008; 14:2321-32. [PMID: 19093009].
17. Wang T, Waters CT, Rothman AM, Jakins TJ, Romisch K, Trump D. Intracellular retention of mutant retinoschisin is the pathological mechanism underlying X-linked retinoschisis. Hum Mol Genet 2002; 11:3097-105. [PMID: 12417531].
18. Wu WW, Molday RS. Defective discoidin domain structure, subunit assembly, and endoplasmic reticulum processing of retinoschisin are primary mechanisms responsible for X-linked retinoschisis. J Biol Chem 2003; 278:28139-46. [PMID: 12746437].
19. Riveiro-Alvarez R, Trujillo-Tiebas MJ, Gimenez-Pardo A, Garcia-Hoyos M, Lopez-Martinez MA, Aguirre-Lamban J, Garcia-Sandoval B, Vazquez-Fernandez del Pozo S, Cantalapiedra D, Avila-Fernandez A, Baiget M, Ramos C, Ayuso C. Correlation of genetic and clinical findings in Spanish patients with X-linked juvenile retinoschisis. Invest Ophthalmol Vis Sci 2009; 50:4342-50. [PMID: 19324861].
20. Hewitt AW, FitzGerald LM, Scotter LW, Mulhall LE, McKay JD, Mackey DA. Genotypic and phenotypic spectrum of X-linked retinoschisis in Australia. Clin Experiment Ophthalmol 2005; 33:233-9. [PMID: 15932525].
21. Karpe G. CHAPTER IV.: The electroretinogram under pathological conditions. Acta Ophthalmol (Copenh) 1946; 24:69-113. .
22. Heckenlively JR, Arden GB. Principles and Practice of Clinical Electrophysiology of Vision. 2nd ed: Cambridge, Mass.: MIT Press; 2006.
23. Renner AB, Kellner U, Fiebig B, Cropp E, Foerster MH, Weber BH. ERG variability in X-linked congenital retinoschisis patients with mutations in the RS1 gene and the diagnostic importance of fundus autofluorescence and OCT. Doc Ophthalmol 2008; 116:97-109. [PMID: 17987333].
24. Vincent A, Robson AG, Neveu MM, Wright GA, Moore AT, Webster AR, Holder GE. A phenotype-genotype correlation study of X-linked retinoschisis. Ophthalmology 2013; 120:1454-64. [PMID: 23453514].
25. George ND, Yates JR, Moore AT. X linked retinoschisis. Br J Ophthalmol 1995; 79:697-702. [PMID: 7662639].
26. George ND, Yates JR, Moore AT. Clinical features in affected males with X-linked retinoschisis. Arch Ophthalmol 1996; 114:274-80. [PMID: 8600886].
27. Thobani A, Fishman GA. The use of carbonic anhydrase inhibitors in the retreatment of cystic macular lesions in retinitis pigmentosa and X-linked retinoschisis. Retina 2011; 31:312-5. [PMID: 20966823].
28. Khandhadia S, Trump D, Menon G, Lotery AJ. X-linked retinoschisis maculopathy treated with topical dorzolamide, and relationship to genotype. Eye (Lond) 2011; 25:922-8. [PMID: 21527955].
29. Genead MA, Fishman GA, Walia S. Efficacy of sustained topical dorzolamide therapy for cystic macular lesions in patients with X-linked retinoschisis. Arch Ophthalmol 2010; 128:190-7. [PMID: 20142541].
30. Walia S, Fishman GA, Molday RS, Dyka FM, Kumar NM, Ehlinger MA, Stone EM. Relation of response to treatment with dorzolamide in X-linked retinoschisis to the mechanism of functional loss in retinoschisin. Am J Ophthalmol 2009; 147:111-5. [PMID: 18834580].
31. Wolfensberger TJ, Mahieu I, Jarvis-Evans J, Boulton M, Carter ND, Nogradi A, Hollande E, Bird AC. Membrane-bound carbonic anhydrase in human retinal pigment epithelium. Invest Ophthalmol Vis Sci 1994; 35:3401-7. [PMID: 8056514].
32. Wolfensberger TJ. The role of carbonic anhydrase inhibitors in the management of macular edema. Doc Ophthalmol 1999; 97:387-97. [PMID: 10896355].

Articles are provided courtesy of Emory University and the Zhongshan Ophthalmic Center, Sun Yat-sen University, P.R. China. The print version of this article was created on 28 April 2015. This reflects all typographical corrections and errata to the article through that date. Details of any changes may be found in the online version of the article.